

**Design and numerical-phase analysis of an SPR system for direct
detection of SARS-CoV-2 virus in pharyngeal swab solution**

*Yansheng Liu^{*a}, Junpeng Deng^{a,b}, Xiaobo Jia^{*a}, Jin Zhou^a, Hongli Li^a, Xiaohong
Wang^a, Yating Chen^a, Zhenle Qin^a, Zhichen Jin^c, and Guofu Wang^a*

^a School of Electronic Engineering, Guangxi University of Science and Technology,
No.2, Wenchang Road, Liuzhou City, 545006, Guangxi, China

^b School of Physics and Optoelectronic Engineering, Guangdong University of
Technology, Guangzhou, China

^c Department of NanoEngineering, University of California San Diego, La Jolla, CA
92093, US

* Corresponding authors (Yansheng Liu: yansheng.liu@gxust.edu.cn; Xiaobo Jia:
xiaobojia@163.com)

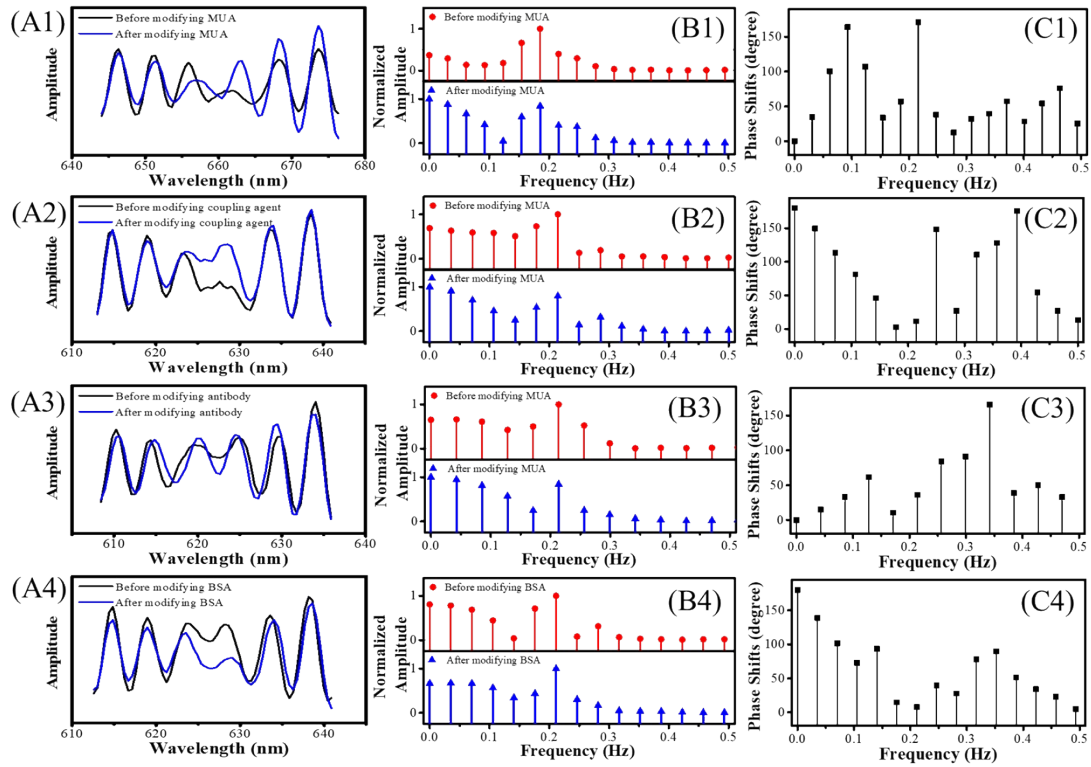


Figure S1. (A1) to (A4) are centralized the SPR spectral interferograms of functionalization of 11-MUA, coupling agents, SARS-CoV-2 antibodies, and BSA. The SPR spectral interferograms are obtained by using the same solvent before and after the functionalization of molecules. (B1) to (B4) are the derived frequency domain results from the interferograms by using WFT. The amplitude of frequencies is normalized and the frequency larger than 0.52 has been omitted because their amplitude is smaller than 0.35 which indicates that they are not the prominent components consisting of the SPR spectral interferograms. (C1) to (C4) are the derived phase shifts $\Delta\phi_f$ of each frequency. The value of $\Delta\phi_f$ of each frequency is normalized from 0° to 360° .

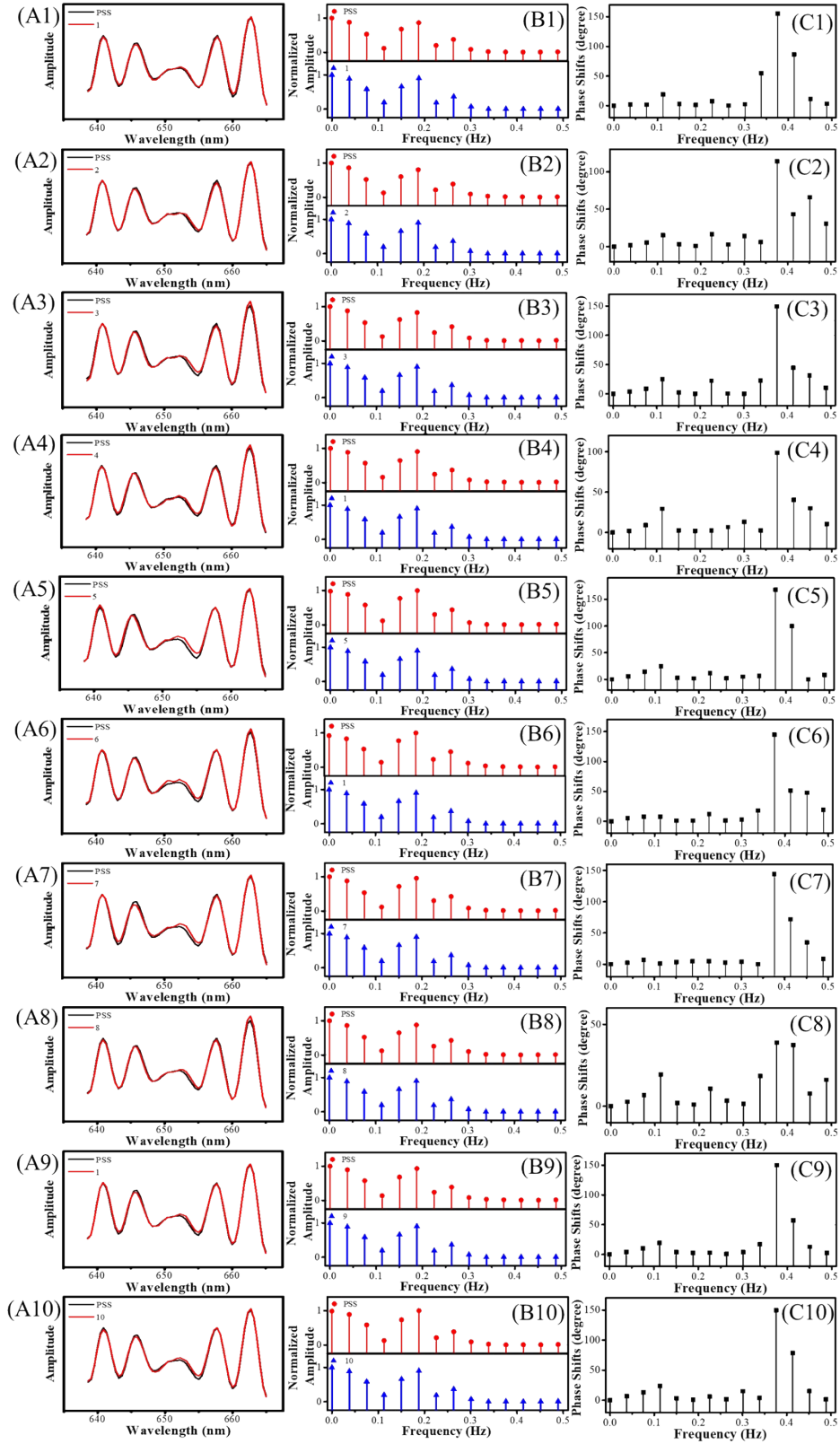


Figure S2. (A1) to (A10) are 10 continuously measured SPR spectral interferograms using PSS as the analyte where the first collected interferogram is used as a reference. (B1) to (B10) are the derived frequency domain results calculated from the interferograms by using WFT. (C1) to (C10) are the derived phase shifts $\Delta\phi_f$ for each

frequency. The value of $\Delta\phi_f$ of each frequency is normalized from 0° to 360° .

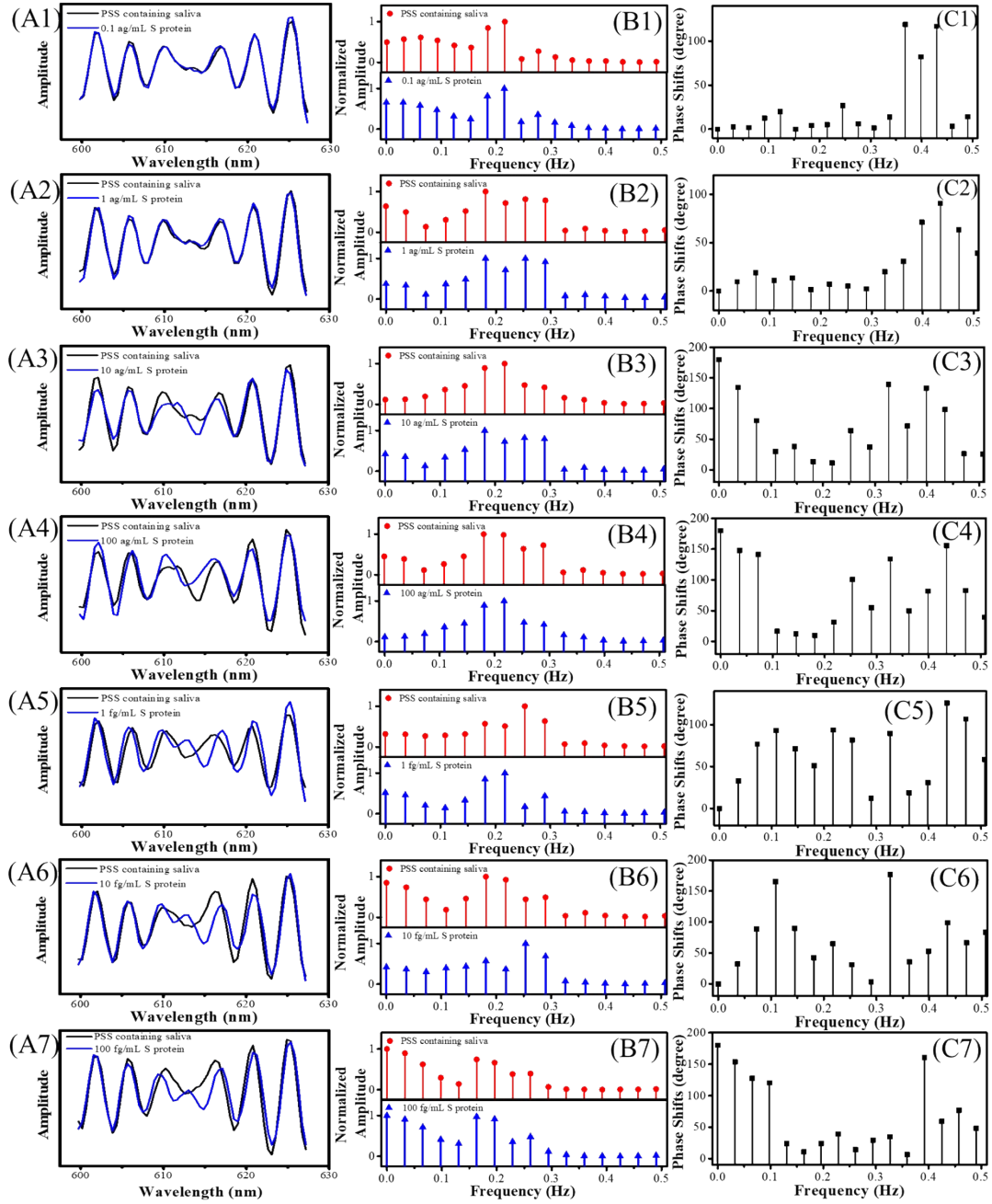


Figure S3. (A1) to (A7) are centralized SPR spectral interferograms of detecting SARS-CoV-2 S protein in PSS containing saliva with varying concentrations. The interferograms are cut at the SPR resonance wavelength. (B1) to (B7) are the derived frequency domain results from the interferograms by using WFT. (C1) to (C7) are the derived phase shifts $\Delta\phi_f$ of each frequency. The value of $\Delta\phi_f$ of each frequency is normalized from 0° to 360° .

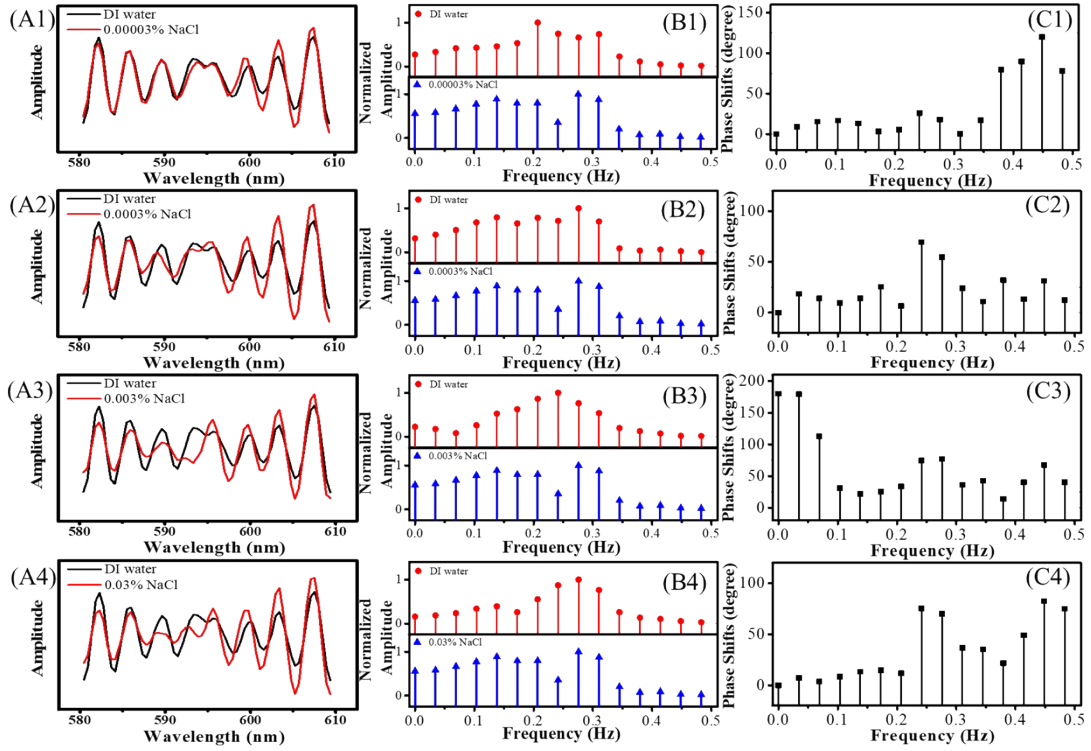


Figure S4. (A1) to (A4) are centralized SPR spectral interferograms of detecting NaCl solution in DI water with varying concentrations. The interferograms are cut at the SPR resonance wavelength. (B1) to (B4) are the derived frequency domain results from the interferograms by using WFT. (C1) to (C4) are the derived phase shifts $\Delta\phi_f$ of each frequency. The value of $\Delta\phi_f$ of each frequency is normalized from 0° to 360° .

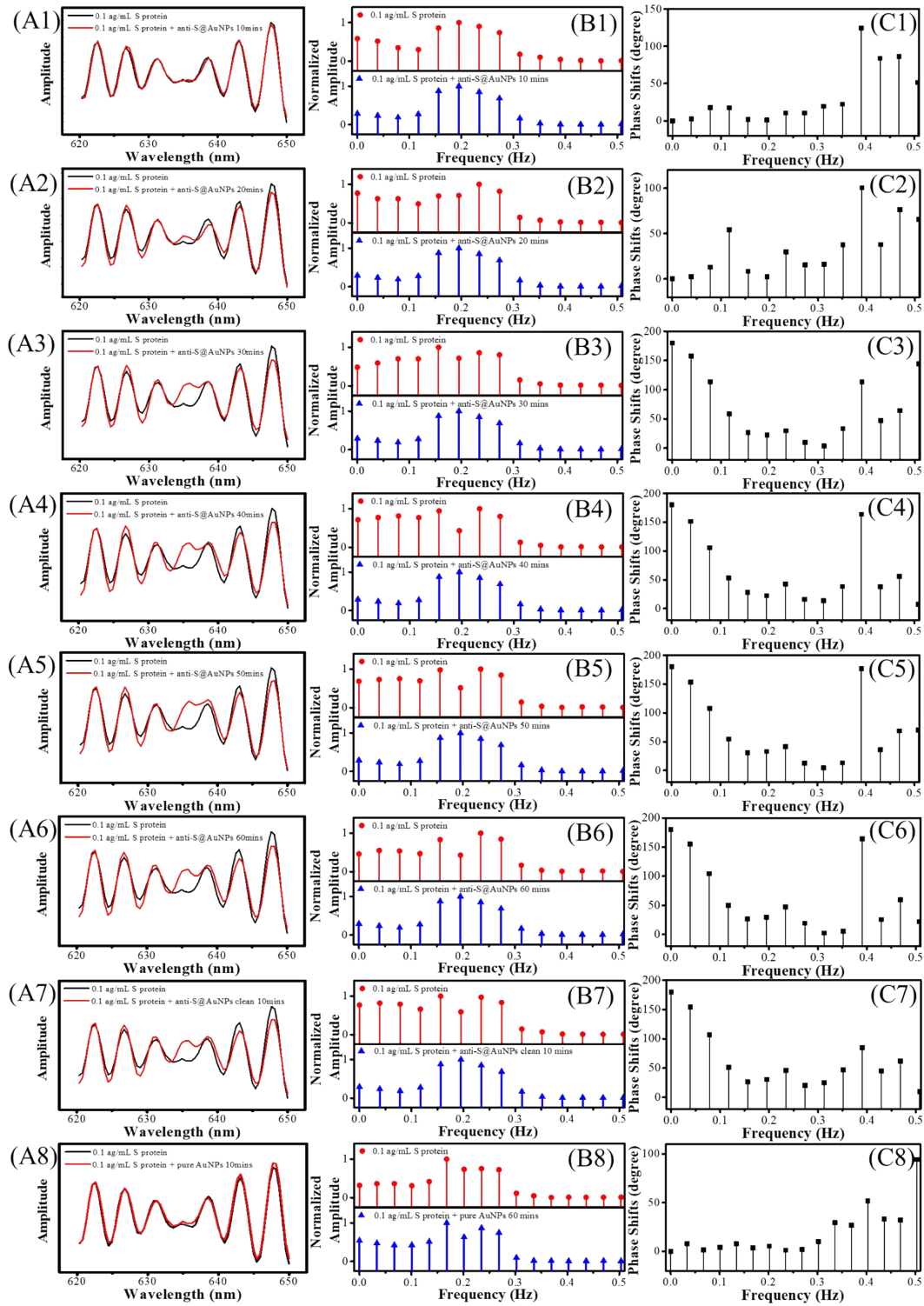


Figure S5. (A1) and (A8) are centralized SPR spectral interferograms of detecting SARS-CoV-2 S protein which is obtained from sandwich sensing surfaces formed by the pure AuNPs and anti-S@AuNPs. (B1) and (B8) are the derived frequency domain results from the interferograms by using WFT. (C1) to (C8) are the derived phase shifts $\Delta\phi_f$ of each frequency. The value of $\Delta\phi_f$ of each frequency is normalized from 0° to 360° .

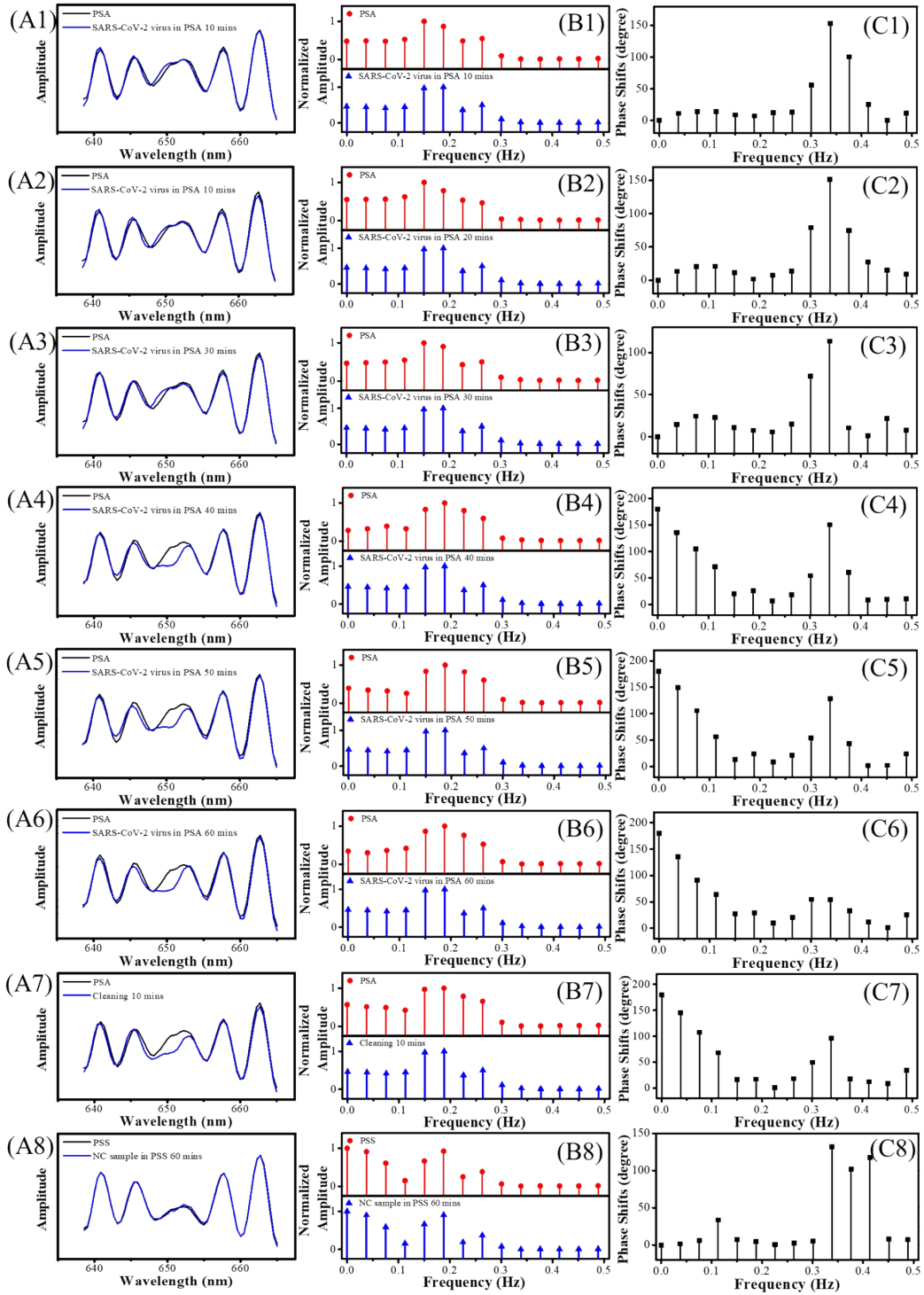


Figure S6. (A1) to (A6) are centralized SPR spectral interferograms of detecting the SARS-CoV-2 virus in PSA with a flow speed of 10 $\mu\text{L}/\text{min}$. (A7) is the centralized SPR spectral interferograms of cleaning the sensing surface by using PSA. (A8) is centralized SPR spectral interferograms of detecting NC samples in PSS. (B1) to (B8) are the derived frequency domain results from the interferograms by using WFT. (C1) to (C8) are the derived phase shifts $\Delta\phi_f$ of each frequency. The value of $\Delta\phi_f$ of each

frequency is normalized from 0° to 360° .